

## Pressure dependence of the *c*-axis resistivity of graphite

C. Uher, R. L. Hockey,\* and E. Ben-Jacob

*Department of Physics, The University of Michigan, Ann Arbor, Michigan 48109-1120*

(Received 2 September 1986)

The *c*-axis resistivity of highly oriented pyrolytic graphite has been measured from 2 to 300 K under hydrostatic pressures of up to 40 kbar. A resistivity peak near 40 K, typical for this type of graphite at ambient pressure, rapidly diminishes with increasing pressure but does not shift its position with respect to temperature. This observation suggests that the origin of the resistivity peak is not in a strong electron-phonon interaction but is associated with a particular structural matrix of these artificially produced graphites. A model is proposed, based on tunneling between microcrystallites, which accounts for the peculiar temperature and pressure dependence of the resistivity.

### I. INTRODUCTION

Graphite is an excellent example of a layered semimetal. Its high structural anisotropy not only governs the physical properties, but it also makes this material the favored matrix for the production of intercalation compounds. While the in-plane transport properties of graphite show an expected metallic character which is reasonably well understood,<sup>1,2</sup> the carrier transport across the graphitic planes is a contentious issue. On purely band-structure considerations the *c*-axis transport should show metallic features, though the effective mass in this case would be about a factor of 100 higher than the in-plane effective mass. This seems to be the case in the best-quality single crystals (both natural<sup>3</sup> and the so-called Kish graphite<sup>4</sup>) where the ratio of the *c*-axis to in-plane resistivities,  $\rho_c/\rho_a$ , is about 100 and the temperature coefficient of resistivity (TCR) is positive, at least below 200 K. On the other hand, the *c*-axis resistivity of the best synthetically produced graphites is about 2 orders of magnitude higher and shows a peculiar temperature dependence<sup>5,6</sup> whereby  $\rho_c$  has a negative TCR down to about 40 K which, at still lower temperatures, gives way to a metallic (positive TCR) dependence. Similar temperature dependence is observed also on exfoliated graphites in both in-plane and *c*-axis configurations<sup>7</sup> and on graphite fibers.<sup>8</sup> Models which have been put forward to explain this unusual resistivity variation are basically of two types: those arguing in terms of the defect structure of graphite,<sup>6,9,10</sup> and those favoring the existence of a strong coupling between the charge carriers and phonons, specifically via the longitudinal acoustic *c*-axis mode.<sup>11,12</sup>

In order to ascertain what effect, if any, the phonons play in the *c*-axis transport of graphite, we have undertaken high-pressure studies of the temperature-dependent resistivity on highly oriented pyrolytic graphite (HOPG) at pressures up to about 40 kbar. The measurements represent the first attempt to extend the study of graphite resistance under high pressure to low temperatures. Previous investigations of graphite which inquired into the change of resistance with pressure were limited to the

room-temperature conditions.<sup>13</sup> In this paper we describe our experimental technique and the results we have obtained, and propose a model which accounts for the peculiar behavior of the *c*-axis transport.

### II. EXPERIMENTAL TECHNIQUE

While it is not absolutely necessary to use truly hydrostatic conditions when making measurements on highly anisotropic materials such as graphite, it is, nevertheless, satisfying and adds to the confidence one has in the data when such conditions are actually achieved. Nowadays, a standard way to do so is to use either a piston-cylinder apparatus or a diamond-anvil cell. Since we were interested in extending the measurements to relatively high pressures and a wide range of temperatures, we have opted for the latter technique.

Our cell, shown in Fig. 1, is a very simple version of the Merrill-Bassett cell and it can readily be attached to a conventional liquid-helium cryostat. The cell is made from Be-Cu alloy and a pair of rather large ( $\frac{1}{3}$  and  $\frac{1}{5}$  karat) diamonds is centered over a small optical-access hole and held in place with a tiny amount of Stycast. In order to cause a relatively small deformation on the face of a gasket where the wires are brought out, the diamond which presses on this face has an area about 25% larger than the other diamond. Gaskets were made mostly from Be-Cu with a small central hole for the sample and four prepressed slots for wires. A standard 3:1 mixture of methanol-ethanol is used as a pressure-transmitting fluid. Pressure is locked in by means of three stainless-steel screws. The actual compression procedure is carried out in a highly aligned vise in which the cell is clamped and the screws are merely tightened in position. The working pressure is determined by the fluorescence technique<sup>14,15</sup> using ruby powder sprinkled around the sample. The cell itself was tested to pressures in excess of 60 kbar. For the temperature-dependent pressure scans, it is essential to know the pressure change on cooling the cell below 300 K. This we have tested in a special liquid-nitrogen Dewar made from glass and provided with high-optical-quality

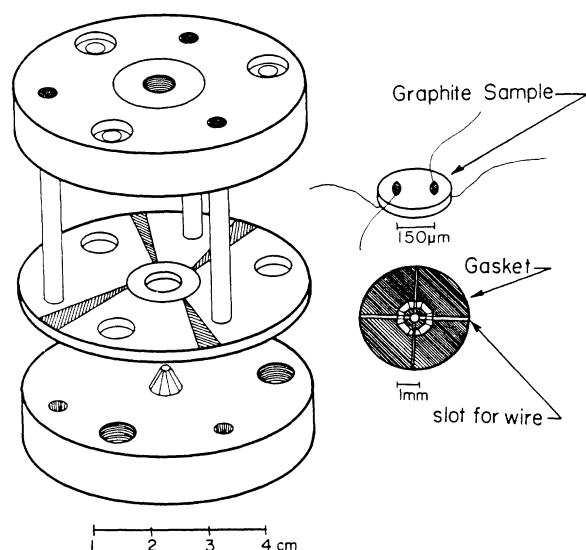


FIG. 1. Schematic drawing of the diamond anvil cell for four-probe resistance measurements under hydrostatic pressure.

windows. Using the known temperature shift of the ruby line at fixed pressures,<sup>16</sup> we estimate that on cycling the cell from 300 K down to 77 K (and surely down to 4 K since thermal expansion below 77 K is very small) the pressure changes by less than 5%.

A crucial consideration in any high-pressure resistivity measurements is how to bring out the wires without guillotining them on or shorting them against the gasket. We stress here that if the resistivity data are intended to provide useful information on the *transport processes*, it is essential that they be done using a four-probe technique, either dc or ac. Two-probe high-pressure measurements, while adequate for the study of, e.g., phase transitions where changes of several orders of magnitude are likely to be encountered, are not appropriate for the present investigations. The method which we found satisfactory is to prepress slots in the gasket in positions where the wires will be located and paint them with a thin layer ( $\sim 10 \mu\text{m}$ ) of epoxy which gives a protective insulation. After the sample is mounted with its connecting leads lying in the slots, an additional thin epoxy coating is applied. Typically, three different pressure points can be obtained on a given sample before the wires are severed or shorted. To cover the range of pressures up to 40 kbar, we have used six identical samples of HOPG. They were carefully cut from a single sheet of HOPG into small disks of  $300 \mu\text{m}$  diameter and  $50\text{--}75 \mu\text{m}$  thickness by a fine air-abrasive jet. By measuring the resistivity of all six samples at zero pressure from 300 K down to 4 K, we have checked that their ambient pressure behavior is identical. Connecting leads of fine copper wire ( $25 \mu\text{m}$  diameter) were attached with the aid of a silver-loaded epoxy. Great care was used to make sure that the current and voltage contacts were spatially separated in order to avoid contact

resistance problems. We used a dc current of  $10 \mu\text{A}$  and the voltage was monitored by a Keithley 181 nanovoltmeter.

### III. RESULTS

The resistivity  $\rho_c$  as a function of temperature, as measured at fixed pressures, is shown in Fig. 2. The numbers above the curves indicate the pressure in kbar. The data are corrected for the thermal expansion and compressibility of graphite along the *c*-axis. The curve at zero pressure is virtually identical with the data of Morgan and Uher<sup>6</sup> and is typical of the *c*-axis resistivity of the best pyrolytic graphites. Its most notable feature, and from the theoretical point of view the most controversial one, is a pronounced maximum near 40 K. It should be stressed that the high-temperature behavior is not a simple activation process which might arise from an enhanced carrier concentration due to the increasing band overlap with temperature. In fact, in the case of exfoliated graphites which show a similar behavior, Uher and Sander<sup>7</sup> were able to fit the high-temperature data to a variable-range hopping model with an exponent of  $\frac{1}{4}$ ; however, this was not possible in the present case. At low temperatures, on the other hand, metal-like features are notable with the

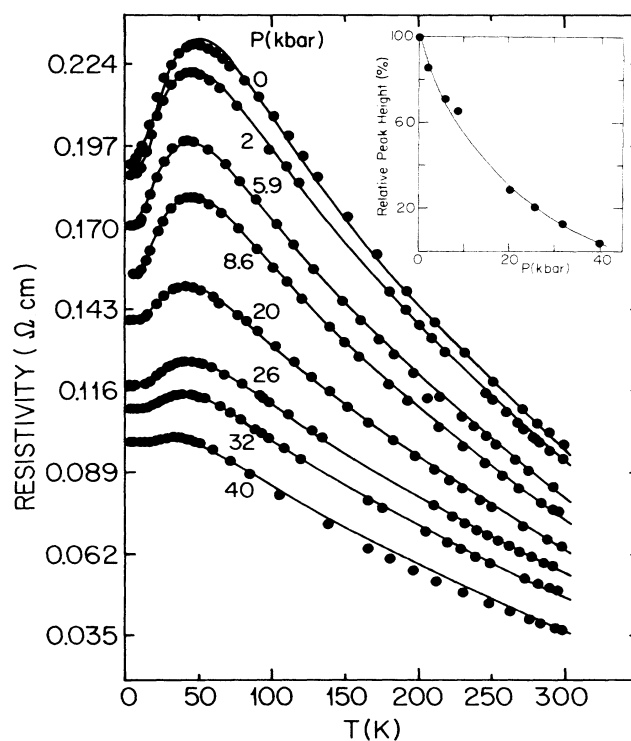


FIG. 2. Temperature dependence of the *c*-axis resistance of HOPG at fixed pressures (indicated in kbars on each curve). The solid curves represent theoretical fits using Eq. (8). In the inset is shown the suppression of the resistivity peak with applied pressure plotted as a percentage of the zero-pressure peak height.

temperature-independent resistivity (impurities, defects) dominating below 5 K and a phonon-limited resistivity at higher temperatures. Some of the theories<sup>11,12</sup> which attempt to explain this strange temperature dependence invoke a coupling of the electron motion to a soft phonon mode. On the basis of our high-pressure data we argue that it is very unlikely that such soft phonon modes play any significant role in the *c*-axis transport. Had they been effective, we would have expected a large stiffening of the modes at high pressures which should lead to a pronounced shift of the resistivity maxima to higher temperatures. This is not what is observed in Fig. 2. While the pressure has a significant effect on the magnitude of the resistivity, the position of the maximum is virtually unchanged up to the highest pressures used. If anything, the maximum on the 40-kbar curve seems to indicate a very small ( $\sim 5$  K) shift to lower temperatures.

A very striking feature of the curves shown in Fig. 2 is a suppression of the resistivity peak with increasing pressure. In the inset of Fig. 2 we show this trend versus pressure by plotting the peak height, defined as the difference between a resistivity value at 2 K and at the temperature corresponding to maximum resistivity, both taken at the same fixed pressure. We note that the peak virtually disappears at pressures in excess of 40 kbar. The mean free path (MFP) established from our *c*-axis resistivity at ambient conditions is about 2.5 Å. Such a small value undoubtedly leads to the breakdown of Boltzmann-type transport, and it is thus not surprising that the TCR is negative. On application of pressure the MFP increases and at 40 kbar and 300 K reaches a value of about 7 Å.

We wish to note that in those cases where we have released the pressure and rechecked the zero-pressure behavior of the resistivity, we have never detected any damage to samples due to the application of pressure as would have been manifested by the change in the magnitude or the profile of the resistivity curves in comparison to the original zero-pressure run. The old Bridgman's quote that graphite is nature's best spring is, in this context, very relevant.

To touch base with the existing high-pressure measurements made at 300 K, we show in Fig. 3 the percentage change in the magnitude of resistivity with pressure at ambient temperature. The dashed line here represents a consensus among several high-pressure *c*-axis investigations<sup>17-19</sup> up to about 10–15 kbar. It is clear that in this pressure range our data are in excellent agreement with the previous measurements. Deviations from the straight line above 15 kbar are typical for this pressure range and arise from the nonlinear pressure dependence of the wave-function overlap parameters  $\gamma$  characterizing the band structure of graphite. The best fit to our data over the pressure range up to 40 kbar yields the equation

$$R(P) = R_0(1 - 0.0276P + 0.0003P^2), \quad (1)$$

where  $P$  is in kbar.

#### IV. DISCUSSION

We have already noted that our experimental data do not support any of the theories of *c*-axis transport which

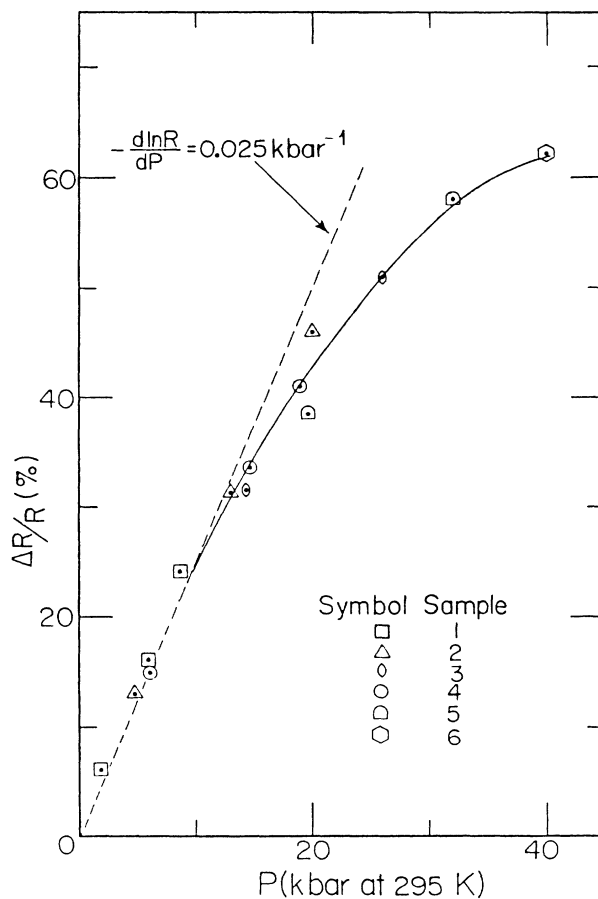


FIG. 3. Pressure dependence of the room-temperature *c*-axis resistivity of our HOPG samples. A dashed line represents a logarithmic pressure derivative established by previous workers for  $P \leq 10$  kbars.

rely on a strong carrier-phonon interaction through either the carrier self-trapping or via a soft phonon mode. In all such circumstances one would expect a shift of the resistivity maximum to higher temperatures as the pressure increases, the trend which is not supported by the observations. Consequently, we believe that the overriding effect on the *c*-axis transport of the artificially produced graphite comes from the structural idiosyncrasy of these materials.

Electron diffraction studies<sup>20</sup> on the best synthetic graphites such as HOPG used here indicate regions of nearly perfect material separated by grain boundaries. The crystallites extend for typically  $\geq 1 \mu\text{m}$  in the basal plane and  $\sim 0.1 \mu\text{m}$  in the *c* direction. Since the distance between graphitic layers is 3.35 Å, an average crystallite spans over some 300 layers. Crystalline regions on either side of the boundaries are rotated with respect to each other and may be tilted by a small angle, less than  $0.5^\circ$  in the best HOPG. Boundaries between the crystallites can be described in terms of arrays of dislocations.<sup>21</sup> It is well known that these dislocations have a tendency to split into

partial dislocations which then enclose a stacking region with the ...*ABC*... stacking sequence symptomatic of rhombohedral graphite. In principle, such stacking faults could act as strongly reflecting barriers and greatly impede the carrier motion in the *c* direction. This, in fact, is the essence of the theory of Ono.<sup>9</sup> Unfortunately, this model predicts the wrong temperature dependence for the *c*-axis resistivity.

If we assume an even more drastic effect of the stacking faults on the charge carriers, namely that they localize them in the basal planes,<sup>22</sup> this is not without difficulties either. First, one would expect to observe some kind of a phonon-assisted hopping transport. However, our attempt to fit the resistivity to the variable-range hopping model has met with little success. Furthermore, our supplemental ac resistance measurements do not show evidence for the characteristic  $\omega^n$  frequency dependence expected for hopping and other activated processes common to disordered materials. In fact up to  $2 \times 10^6$  cycles/sec, the highest frequency available to us, we observe no change from the dc resistivity. Microwave studies on the *c*-axis resistivity by Dresselhaus *et al.*<sup>23</sup> arrive at the same conclusion.

Motivated by the experimental results of this study and guided by the microstructural configuration of HOPG, we propose a model of the *c*-axis transport based on tunneling between the crystallites, in addition to the spatially limited paths of metal-like conduction. We write the total conductivity  $G$  as a superposition of the two mechanisms

$$G = G_T + G_M, \quad (2)$$

where  $G_T$  is the conductivity due to tunneling and  $G_M$  is the metallic part of conduction acting in parallel with  $G_T$ . Although we have not established a specific mechanism of  $G_M$  one possibility is a series of overlapping planar defects (e.g., grain boundaries, cracks) which allow a parallel conduction channel for the motion of electrons along the *c*-axis. In any event, guided by our experimental observations at low temperatures, we make a reasonable assumption that the *mechanism* of the metallic (i.e., phonon-limited) conduction in HOPG should be the same as in single-crystalline graphites (SCG's); after all, they have the same band structure and carrier and phonon densities. We then fit the temperature dependence of the best SCG's which we have measured<sup>24</sup> and which show metallic character throughout the entire temperature range. Typical data for the high-quality SCG samples are shown in Fig. 4; for  $T \leq 70$  K the temperature dependence of the conductivity is well described by the expression

$$G_M = \frac{b}{T^2 + c}, \quad (3)$$

where  $b$  and  $c$  are fitting parameters. We assume that this same functional dependence on temperature (with, of course, different parameters  $b$  and  $c$ ) applies also to HOPG. As the contribution of  $G_M$  to the total conductivity of HOPG above liquid-nitrogen temperature is progressively diminishing, the error made by extending the formula (3) above 100 K, where it becomes a less satisfactory fit, is small.

To estimate the contribution of tunneling to the con-

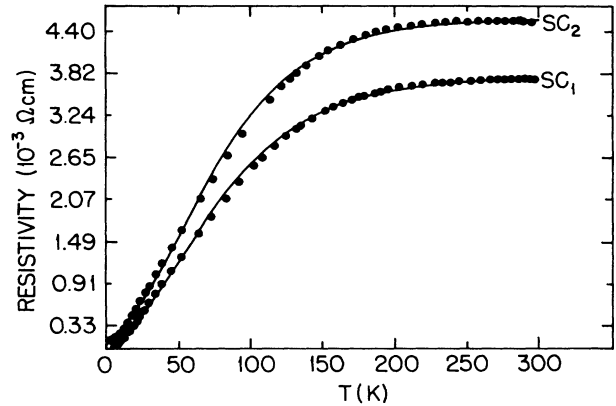


FIG. 4. *c*-axis resistivity as a function of temperature for the high-quality single-crystal graphite samples SC<sub>1</sub> and SC<sub>2</sub>. Residual resistivity ratio (RRR) for the two samples are 62 and 75, respectively. The solid curves represent fits to the data with the formula  $\rho = (b/T^2 + a/T + \gamma)^{-1} + \delta$ . For  $T \leq 70$  K, a simpler expression  $\rho = (b/T^2)^{-1} + \delta = (T^2 + c)/b$ , introduces a less than 2% difference in comparison to the original formula given above.

ductance we follow Stratton<sup>25</sup> and Simmons<sup>26</sup> and calculate the current-voltage characteristics for a conductor-insulator-conductor junction. With use of the notation of Ben-Jacob *et al.*,<sup>27</sup> the dimensionless probabilities per unit time of transferring an electron from right to left,  $P_{rl}$ , and from left to right,  $P_{lr}$ , are given by

$$P_{rl} = \int T(E)D(E)f_r(E)[1 - f_l(E + eV)]dE, \quad (4)$$

$$P_{lr} = \int T(E)D(E)f_l[1 - f_r(E - eV)]dE,$$

where  $V$  is the voltage across the junction,  $f_r$  ( $f_l$ ) are the equilibrium Fermi distribution functions on the right (left) side, and  $T(E)$  is the tunneling probability of an electron at energy  $E$  above the Fermi level on the right. The latter is calculated using the Wentzel-Kramers-Brillouin approximation assuming, for simplicity, a square potential barrier  $U(X)$  extending from  $X_r$  to  $X_l$ ,

$$T(E) \sim \exp \left[ -\frac{4\pi}{h} \int_{X_r}^{X_l} \{2m[U(X) - E]\}^{1/2} dx \right], \quad (5)$$

where  $m$  is the effective mass of the electron. With use of this formula the net current through the barrier is

$$I = \frac{e}{\tau} \int T(E)D(E)[f_r(E) - f_l(E + eV)]dE, \quad (6)$$

where the relaxation time  $\tau$  is a phenomenological constant representing the  $RC$  time constant of the junction, assuming the density of states stays constant. At  $T=0$ , the tunneling part of the conductance  $\sigma_T(0)$  is trivially obtained from Eq. (6). The temperature dependence enters through the Fermi distribution functions. At low temperatures, to the leading order, the conductance is of the form

$$\sigma_T(T) = \sigma_T(0) + gT^2, \quad (7)$$

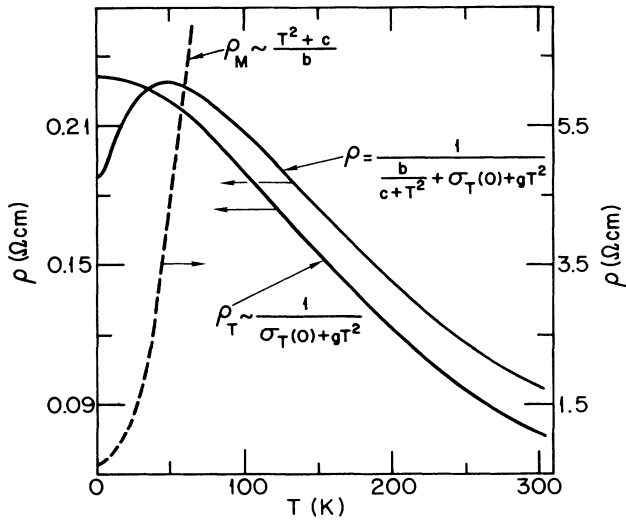


FIG. 5. Temperature dependence of the *c*-axis resistivity due to tunneling, metallic contribution to the resistivity, and their combined resistivity. Appropriate scales are indicated by the arrows.

where  $g$  is a constant dependent on the barrier geometry.

The overall temperature dependence of the conductivity is, combining Eqs. (3) and (7),

$$\sigma(T) = \sigma_T(0) + gT^2 + \frac{b}{T^2 + c}. \quad (8)$$

Temperature dependence of the *c*-axis resistivity at ambient pressure due to tunneling, due to extended states, as well as their combined resistivity  $\rho = \sigma^{-1}(T)$ , is shown in Fig. 5. It follows that the experimental data can be fit very well with this model and the appropriate coefficients are given in Table I. It is also clear that tunneling alone is not able to reproduce the low-temperature data and a small metallic contribution acting in parallel is essential here.

Let us now turn our attention to the pressure dependence. For simplicity we can view the barrier as a rectangular one and assume that the dominant role of pressure is to vary the width of the barrier in a way similar to the overall change of the *c*-axis lattice spacing with pressure (compressibility). Such a change would result in a modification of the tunneling probability  $T(E)$  through

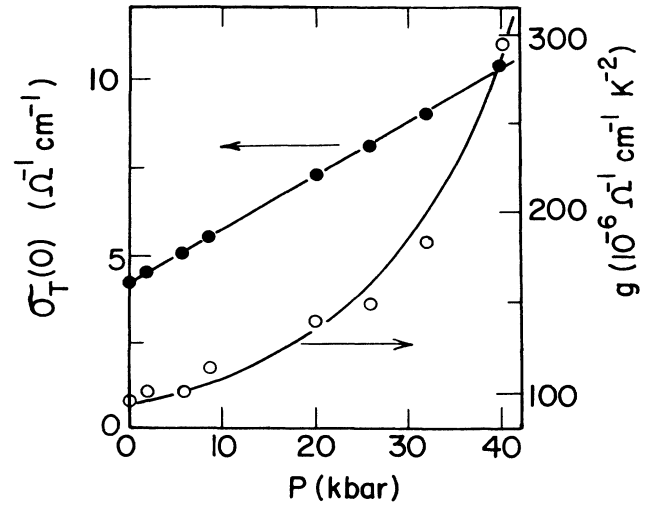


FIG. 6. Pressure variation of the parameters  $\sigma_T(0)$  and  $g$  obtained from the best fits to the data of Fig. 2.

the change in the boundary conditions of Eq. (5) and, hence,  $g$  will be modified correspondingly. Adjusting the parameters of Eq. (8) for increasing pressure, the excellent fits in Fig. 2 were realized for each pressure run. From these fits we found that the coefficients  $b$  and  $c$  are relatively independent of pressure in comparison to the coefficients  $\sigma_T(0)$  and  $g$ , thus indicating that the dominant effect of pressure is the enhancement of the tunneling mechanism. Pressure variation of the parameters  $\sigma_T(0)$  and  $g$  obtained from the fits to the data in Fig. 2 is shown in Fig. 6. We note that  $\sigma_T(0)$  varies linearly with pressure while a parabola appears to be a reasonable fit to the pressure dependence of the coefficient  $g$ .

While our assumption of a square tunneling barrier may appear to be a simplified picture, the qualitative agreement with the experimental high-pressure data supports our tunneling model. We also note that this model provides a unified framework for understanding the *c*-axis resistivity of both single-crystal graphites (metallic part dominates), HOPG discussed here (both metallic and tunneling mechanisms contributing), and highly disordered graphite materials such as exfoliated graphites (metallic contribution negligible).

#### ACKNOWLEDGMENTS

We are grateful to Professor R. Merlin for making available his laser and spectrometer for pressure calibration of the diamond cell and to Professor R. Clarke for useful discussions concerning the structure of graphites. The work was supported in part by the National Foundation for Low Temperature Physics Grants Nos. DMR-83-04356 and DMR-85-08392 and by the Michigan Memorial Phoenix Project.

TABLE I. Parameters yielding the best fit to the *c*-axis resistivity of HOPG at ambient pressure.

$b$ ( $\Omega^{-1} \text{cm}^{-1} \text{K}^2$ )	$c$ ( $\text{K}^2$ )	$\sigma_T(0)$ ( $\Omega^{-1} \text{cm}^{-1}$ )	$g$ ( $\Omega^{-1} \text{cm}^{-1} \text{K}^{-2}$ )
699	436	4.313	$9.5 \times 10^{-5}$

- \*Present address: Shell Development Company, Houston, TX 77001.
- <sup>1</sup>I. L. Spain, in *Chemistry and Physics of Carbon*, edited by P. L. Walker, Jr., and P. A. Throver (Marcel Dekker, New York, 1980), Vol. 16, p. 119.
- <sup>2</sup>D. T. Morelli and C. Uher, *Phys. Rev. B* **30**, 1080 (1984).
- <sup>3</sup>W. Primak and L. H. Fuchs, *Phys. Rev.* **95**, 22 (1954).
- <sup>4</sup>D. Z. Tsang and M. S. Dresselhaus, *Carbon* **14**, 43 (1976).
- <sup>5</sup>I. L. Spain, A. R. Ubbelohde, and D. A. Young, *Phil. Trans. Soc. London, Ser. A* **262**, 1128 (1967).
- <sup>6</sup>G. J. Morgan and C. Uher, *Phil. Mag.* **B 44**, 427 (1981).
- <sup>7</sup>C. Uher and L. M. Sander, *Phys. Rev. B* **27**, 1326 (1983).
- <sup>8</sup>I. L. Spain, K. J. Volin, H. A. Goldberg, and I. L. Kalnin, *Solid State Commun.* **45**, 817 (1983).
- <sup>9</sup>S. Ono, *J. Phys. Soc. Jpn.* **40**, 498 (1976).
- <sup>10</sup>K. Kawamura, Y. Ouchi, H. Oshima, and T. Tsuzuku, *J. Phys. Soc. Jpn.* **46**, 587 (1979).
- <sup>11</sup>D. A. Young, *Carbon* **6**, 135 (1968).
- <sup>12</sup>Yu. A. Pospelov, *Fiz. Tverd. Tela (Leningrad)* **6**, 1525 (1964) [*Sov. Phys.—Solid State* **6**, 1193 (1964)].
- <sup>13</sup>For a review of high-pressure properties of graphite see R. Clarke and C. Uher, *Adv. Phys.* **33**, 469 (1984), and references therein.
- <sup>14</sup>G. J. Piermarini, S. Block, J. D. Barnett, and R. A. Forman, *J. Appl. Phys.* **46**, 2774 (1975).
- <sup>15</sup>H. K. Mao, P. M. Bell, J. W. Shaner, and D. J. Steinberg, *J. Appl. Phys.* **49**, 3276 (1978).
- <sup>16</sup>D. M. Adams, R. Appleby, and S. K. Sharma, *J. Phys. E* **9**, 1140 (1976).
- <sup>17</sup>Y. Iye, O. Takahashi, S. Tanuma, K. Tsuji, and S. Minomura, *J. Phys. Soc. Jpn.* **51**, 475 (1982).
- <sup>18</sup>I. L. Spain, in *Proceedings of the Conference on Electronic Density of States, 1969*, National Bureau of Standards (U.S.) Publication No. 323, (U.S. G.P.O., Washington, D.C., 1971), p. 717.
- <sup>19</sup>M. L. Yeoman and D. A. Young, *J. Phys. C* **2**, 1742 (1969).
- <sup>20</sup>A. W. Moore, A. R. Ubbelohde, and D. A. Young, *Proc. R. Soc. London, Ser. A* **280**, 153 (1964).
- <sup>21</sup>S. Amelinckx, P. Delavignette, and M. Heerschap, in *Chemistry and Physics of Carbon*, edited by P. O. Walker, Jr. and D. A. Throver (Marcel Dekker, New York, 1965), Vol. 1.
- <sup>22</sup>I. L. Spain, *Proceedings of the International Conference on Physics of Semimetals and Narrow-Band-Gap Semiconductors, Dallas, 1970*, edited by D. L. Carter and R. T. Bate (Pergamon, London, 1971), p. 177.
- <sup>23</sup>M. S. Dresselhaus, private communication in Ref. 9.
- <sup>24</sup>Single-crystal graphites were obtained from calcite deposits at the Gouveneur Talc Mine near Watertown, New York. Each graphite crystal was examined by x rays to check its single-crystalline nature and the highest quality ones were selected for the transport studies.
- <sup>25</sup>R. Stratton, *Phys. Rev.* **125**, 67 (1962).
- <sup>26</sup>G. Simmons, *J. Appl. Phys.* **35**, 2655 (1964).
- <sup>27</sup>E. Ben-Jacob, D. J. Bergman, B. J. Matkowsky, and Z. Schuss, *Phys. Rev. B* **134**, 1572 (1986).